JOURNAL OF MATERIALS SCIENCE 23 (1988) 3248–3253

Strength variations of reaction-sintered SiC heterogeneously containing fine-grained β-SiC

CHANG-BIN LIM, TAKAYOSHI ISEKI
Research Laboratory for Nuclear Reactors, Tokyo Institute of Technology, Ohokayama, Meguro-ku, Tokyo 152, Japan

Strength variations of reaction-sintered SiC were examined to determine the effect of the volume fraction of fine-grained β-SiC domain. The fracture strength significantly decreased with an increase in the volume fraction of the β-SiC domain, and eventually fell to the strength of the β-SiC domain alone. Furthermore, a substantial difference in the crack deflection was found between the indentation microfracture formed in a structure containing fine-grained β-SiC and that in the typical structure of reaction-sintered SiC. This showed that the fracture toughness decreased on account of the β-SiC layer.

1. Introduction

Reaction-sintered SiC is typically fabricated by infiltrating liquid silicon into a mixed green compact of primary α-SiC grains and carbon powder. A certain amount of the newly-formed SiC from the reaction of carbon with liquid silicon is sometimes found as independently nucleated fine-grained β-SiC between the primary α-SiC grains.

Reports related to the presence of this fine-grained β-SiC have been presented by a number of investigators [1–9]. The following areas of investigation were included in the detailed results: (i) characterization of the independently grown β-SiC grains using SEM and TEM techniques [2]; (ii) recrystallization of the β-SiC grains owing to heat-treatment in the presence of molten silicon [3]; (iii) identification of types, distribution condition, and cause of formation of the β-SiC regions [5, 6]. In particular, Sawyer and Page [5] and Ness and Page [6] first stated the definitions that *intergranular* fine-grained β-SiC is a fine-scale and equiaxed material with uniform grain size ($\geqslant 0.5\,\mu m$) which is produced between the original α-SiC grains, and *nodular* fine-grained β-SiC has a uniform or varying grain size ($\leqslant 0.5\,\mu m$) and is produced in the absence of any original α-SiC nucleation sites.

In previous reports by Lim and Iseki [8, 9], it was found that the fine-grained ($0.27\,\mu m$) β-SiC was transported or migrated through liquid silicon as the temperature rose, due to the solution–precipitation mechanism and rearrangement process. Consequently, from the variation of the distribution conditions and the quantities of the intergranular fine-grained β-SiC produced by temperature variations, the formation of the β-SiC could have been due to the higher degree of supersaturated solution of carbon in liquid silicon (in the lower-temperature outer region of the bulk specimen). The nodular fine-grained β-SiC may have appeared after the dissipation of the intergranular fine-grained β-SiC domain. This would have happened once the locally low distribution of the liquid silicon (due to variation in the porosity of the green compact) had made mass transport impossible. It is thought, however, that the small bonded area of grain boundary and the imperfect bonding condition of this fine-grained β-SiC may have affected the mechanical properties of the sintered body.

Much research has already been done on fine-grained β-SiC, but as yet there has been no systematic and quantitative investigation of the strength variations of the reaction-sintered body with changes in the fine-grained β-SiC content. The present study was undertaken, using the specimens described in the previous report [9], to examine the effect of an intergranular fine-grained β-SiC domain on the four-point bending strength of these specimens. A substantial difference in the crack deflection of an indentation microfracture is also shown.

2. Experimental procedure

Reaction-sintered SiC was prepared by the method previously described [9, 10]. The raw materials were α-SiC filler (GC 2000 from Fijimi Kenmazai Kogyo Co. Ltd, Nagoya, grain size $7.9\,\mu m$) and carbon black (Diablack I from Mitsubishi Chemical Industries Ltd, Tokyo, grain size $0.02\,\mu m$). Powders of α-SiC and carbon were mixed in a ratio of 2 : 1, then uniaxially pressed into plates of about 26 mm × 26 mm × 6 mm at 25 MPa in a graphite die. The plates were next isostatically pressed at 260 MPa in thin-walled rubber. The pressed density was about 78 to 85% of the "required density" which was the pressed mixture density to give a theoretically dense SiC [11]. Generally, green compact with about 90% "required density" is used for the fabrication of a reaction-sintered body. The compacts were fired for 30 min in graphite crucibles inside a graphite resistance furnace, at 1450, 1500, 1550 and 1600° C in a vacuum of 0.65 Pa (4.8×10^{-3} torr).

These specimens were sectioned into slices of 26 mm × 4 mm × 2 mm and polished to $1\,\mu m$ in

0022–2461/88 $03.00 + .12

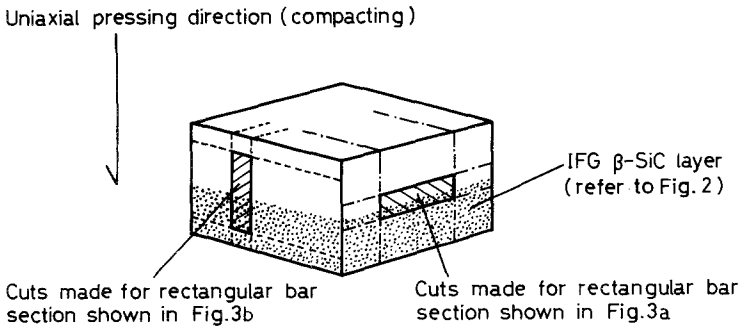

Figure 1 Sintered body configuration and rectangular test specimen sectioning.

the longitudinal direction with the section planes perpendicular or parallel to the original uniaxial pressing direction (Fig. 1).

The densities of the resulting specimens were measured by the Archimedes principle, using water, and elastic modulus determinations of both the typical structure and the intergranular fine-grained β-SiC structure alone (Fig. 2) were made by placing a strain gauge on the surface of the bending test specimen.

The two edges of the tensile surface of the specimens were rounded for fracture strength measurements, and these were carried out in four-point bending with inner span 10 mm and outer span 20 mm, and cross-head speed 0.5 mm min^{-1}.

The indentation microfracture (IM) techniques were applied under a load of 2.9 N for 20 sec, using a Vickers hardness tester. These produced radial/median cracks, primarily at the corners of the indents.

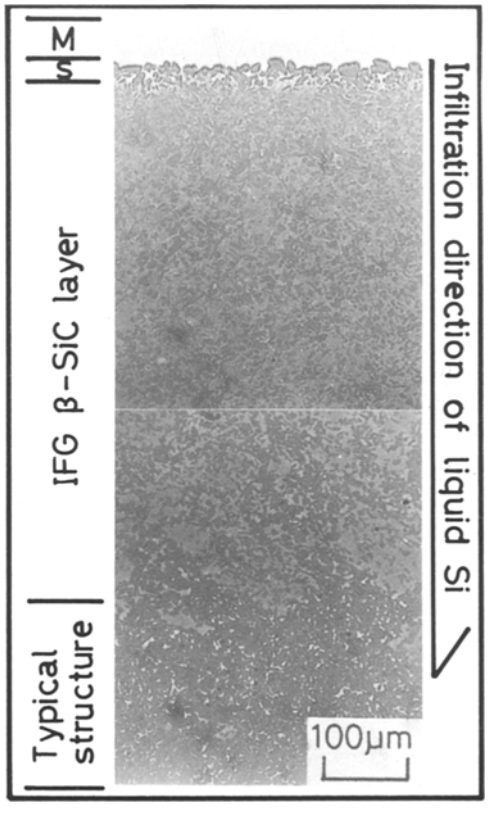

Figure 2 A detail of the microstructure of an unetched polished surface by optical microscopy. The specimen was obtained by sintering at 1450° C for 30 min in a vacuum. (M) molten silicon for reaction, (S) silicon-rich layer.

The polished surface was observed with an optical microscope. The fractured surface was also observed with a scanning electron microscope after free silicon had been removed by HF + HNO_3 etchant.

3. Results and discussion

The bulk density of specimens ranged from 3.08 to 3.11 g cm^{-3}, giving a calculated free silicon of 8.7 to 11.4 wt %, and suggesting that there were almost no pores in the specimens. The ratio of the free silicon in both the intergranular fine-grained β-SiC (hereafter referred to as IFG β-SiC) structure alone and the typical structure is nearly 1 : 1. An optical micrograph of these is shown in Fig. 2. Fig. 2 reveals the evolution along the infiltration or reaction direction of liquid silicon. The white matrix is free silicon, and the grey parts show newly-formed fine SiC grains which are embedded in free silicon. The black angular material is the original α-SiC, or that which is epitaxially bonded to the original α-SiC and newly-formed SiC. It is noteworthy that the sizes of the black angular grains in the IFG β-SiC layer are smaller than those in the typical structure. The specimens of the two types, which were sectioned separately, had nearly the same elastic moduli of 420 GPa (4.2×10^6 kgf cm^{-2}), although that of the typical structure was a little higher.

3.1. Strength variations as a function of volume fraction of IFG β-SiC domain

Both elastic moduli have to be considered when calculating the fracture strength (by four-point bending test) of a material with two different structures as a two-layer composite. In this experiment, however, the bending strength for the rectangular test specimen can be calculated using the general flexure stress formula, since as mentioned above the elastic moduli of both specimens are nearly equal:

$$\sigma = 3Pa/2bd^2 \quad (1)$$

where P is load, a the difference between outer and inner spans, b the width of the specimen and d the thickness.

In the four-point bending strength measurements of bodies sintered at 1450° C for 30 min in a vacuum, the specimens containing the IFG β-SiC domain exhibited strength variations from 590 to 350 MPa (Fig. 3a), or from 520 to 240 MPa (Fig. 3b) as the volume fraction of β-SiC became higher. These specimens contained a total volume of about 5 to 10 vol % nodular fine-grained β-SiC (hereafter referred to as nodule) [5, 6, 9].

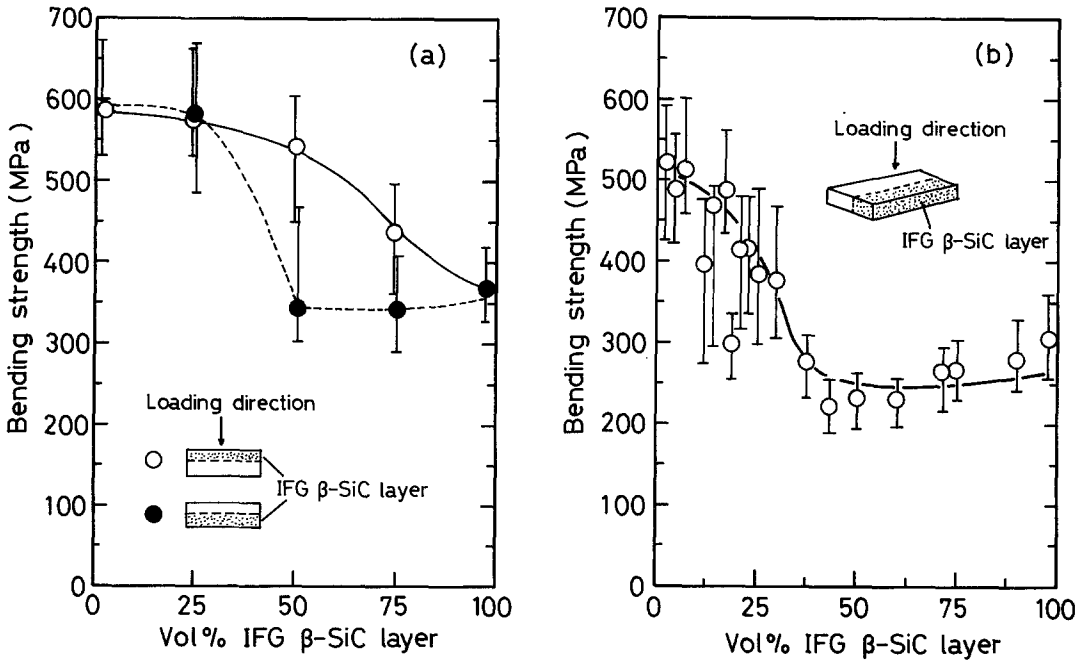

Figure 3 Strength variations as a function of volume fraction of IFG β-SiC domain (layer). IFG β-SiC layer (a) perpendicular and (b) parallel to the loading direction.

In Fig. 3a, when the IFG β-SiC layer was situated at the tensile face, the strength dropped sharply above 25 vol % of IFG β-SiC layer and then became nearly constant. The strength fell more gradually when the typical structure was situated at the tensile face, although it did drop rather rapidly at 75 vol % IFG β-SiC layer. On the other hand, in Fig. 3b, a similar dependence on the percentage of IFG β-SiC layer was also observed for the fracture strength. The fracture strength of the specimen fell gradually with increase in volume fraction of the IFG β-SiC layer to become nearly constant above about 40 vol %. It is not clear whether the differences between the data for the typical structure and the IFG β-SiC structure alone in Figs 3a and b are due to anisotropy by uniaxial pressing of the mixed green compact. Ness and Page [6] reported that modulus-of-rupture data of an extruded specimen of Refel SiC exhibited considerable anisotropy, but in the case of a pressed specimen this would be expected to have little effect. Even for the bending strength of hot-pressed SiC, Iseki *et al.* [12] found no significant influence of the pressing direction on the bending strength. The data for the typical structure in Fig. 3b is similar to that of the similar material Refel SiC [13–15].

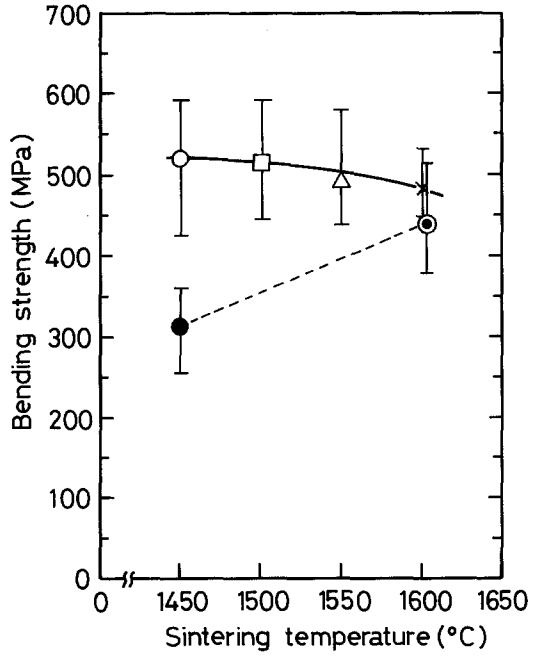

Figure 4 (○, □, △, ×) Strength variations as a function of sintering temperature (heating time 30 min). IFG β-SiC domain removed. (◉) Specimens siliconized at 1450° C and further heat-treated at 1600° C for 30 min in a vacuum; (●) IFG β-SiC structure alone.

The four-point bending strength data for specimens with rising sintering temperature are shown in Fig. 4. It was found that the fracture strength of the IFG β-SiC structure alone increased to 445 MPa due to recrystallization (coalescence) under heat-treatment. The recrystallization in reaction-sintered SiC has already been reported [3, 8]. The reason why the strength of the heat-treated specimen is lower than that of the specimen directly sintered at 1600° C is thought to be as follows: unlike the directly sintered specimen, the recrystallized specimen consists of a polycrystalline structure of small grains; consequently, the number of residual amorphous grain-boundary layers between the accompanying crystals may reduce the fracture strength. Ness and Page [6] reported that SiC : SiC grain boundaries, SiC : SiC epitaxial boundaries and SiC : Si interfaces comprise a thin (1 nm) layer of amorphous SiC with occasional silicide and graphite inclusions. Clarke [16] and Faber and Evans [17] have reported that materials processed using a liquid phase often contain a residual amorphous grain boundary layer, which is often less tough than the accompanying crystals, as exemplified by the silicate phase in HP-SiC.

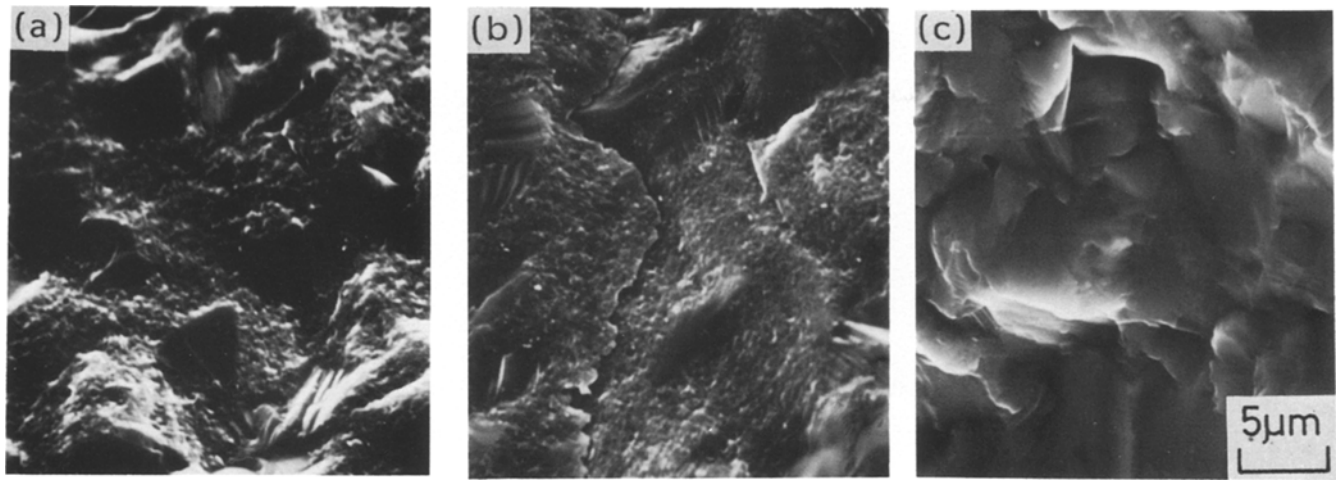

Figure 5 Scanning electron micrographs of fractured surfaces in (a, b) IFG β-SiC domain and (c) typical structure of specimen. Free silicon was etched away with HF + HNO_3.

3.2. Fracture mode by bending test

As mentioned above, the presence of the IFG β-SiC domain (layer) caused a significant volume-fraction-dependent degradation of the sintered-body strength. It is therefore necessary to examine the fracture mode on the fractured surface of the specimen. SEM micrographs of fractured surfaces in the IFG β-SiC domain and the typical structure of a sintered body are shown in Fig. 5. The failure mode in the IFG β-SiC domain which consisted of original α-SiC with fine-grained β-SiC (Fig. 5a), or an epitaxial layer on the original α-SiC with fine-grained β-SiC (Fig. 5b), was primarily intergranular. In contrast, the fracture mode in the typical structure was transgranular and predominantly featureless, although it could be accompanied by partly intergranular fracture (Fig. 5c).

The strength behaviour of two-phase ceramics with a second phase distributed as discrete particles is reasonably well understood in the literatures [18–20]. The strengthening mechanism of dense, highly packed SiC crystals in silicon matrix has also been explained [13]. The fracture in SiC is primarily transgranular [17], but where there are two extreme peaks in the average grain size, as in this experiment, the fracture become predominantly intergranular at small grain boundaries (Fig. 5a). The grain-boundary fracture energy should be less than the transgranular fracture energy (cleavage energy) [21]. This should be especially marked in materials with imperfect grain bonding at grain boundaries. However, provided that the grain bonding condition is sufficiently firm, the grain-boundary fracture energy ought not to decrease so much; considerable reductions in fracture strength should not occur (refer to the data for the heat-treated specimen in Fig. 4). In polycrystalline ceramics, obstacles such as grain boundaries can hinder crack propagation and prevent fracture of the body. The increase in stress for a crack to change direction at a boundary has been analysed by Gell and Smith [22], who showed that increases of factors of 2 to 4 are anticipated for typical polycrystalline arrays.

3.3. Crack deflection of indentation microfracture

Similar trends were observed in Vickers indentation fractures on polished surfaces. Crack deflections of Vickers IM are shown in Fig. 6. The crack traces thus formed reveal the path of a propagating crack and have previously been used to characterize crack–microstructure interactions [17]. The fracture paths in the sintered SiC remain planar throughout propagation. It is notable that the cracks in the IFG β-SiC layer look transgranular, but are actually intergranular (Fig. 6a). Crack deflections in the typical structure (Fig. 6b) are generally more irregular than those in the IFG β-SiC structure (Fig. 6a). The fracture

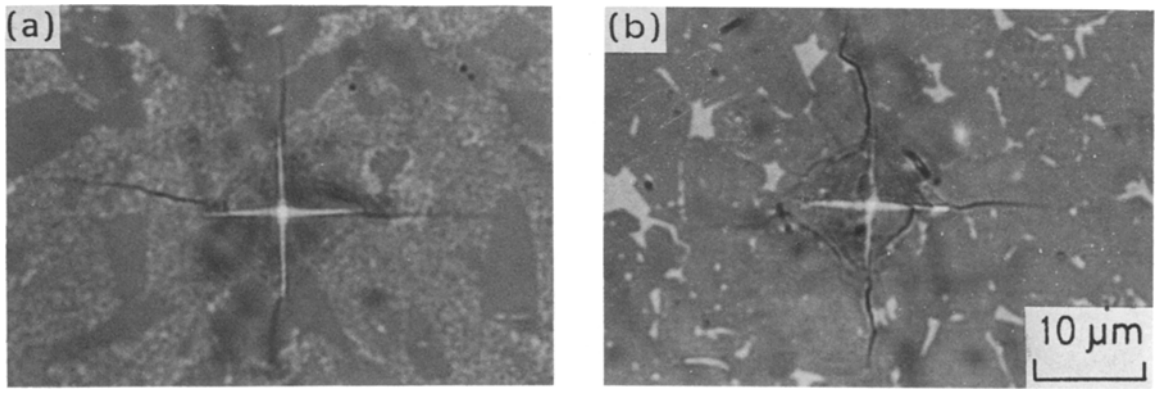

Figure 6 Crack deflections of Vickers indentation microfracture in (a) IFG β-SiC structure and (b) typical structure in reaction-sintered body.

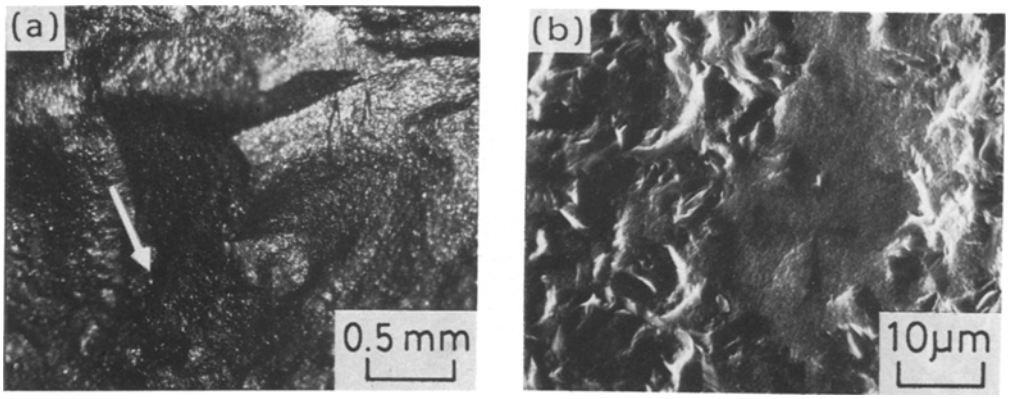

Figure 7 Observation of fractured surfaces. (a) Stereo-optical micrograph; (b) scanning electron micrograph at higher magnification of part of the flaw marked with an arrow in (a).

toughness (K_{Ic}) at room temperature was determined by the IM technique [23, 24] using the equation below [25] which was normalized with sintered SiC:

$$\frac{K_{Ic}}{H_a} = 0.203 \frac{c}{a} \quad (2)$$

The characteristic dimensions of the impression half-diagonal (a) and the radial/median crack length (c) were measured by an optical microscope. The fracture toughness decreased significantly from 4.7 (typical structure: Fig. 6b) to 3.1 MPa $m^{1/2}$ (IFG β-SiC structure: Fig. 6a). This result corresponds to that for the four-point bending strength. In Fig. 6a, the length of vertical crack was shorter than that of the horizontal crack because the larger α-SiC grain became an obstacle to further crack propagation. The effect of grain shape in the β-SiC region must also be considered for crack propagation because this material has equiaxed and uniform grains [5, 6, 9]. In particular, elongated grains (such as rods or discs) should be more effective at toughening than equiaxed grains [17].

3.4. Fracture in structures containing nodule

Fig. 7 shows a fractured surface of a typical structure which contains a total volume of about 5 to 10 vol % nodule. There is a flaw in the vicinity of the nodule, but the overall fractured surface shows indistinct fracture features. If the material has a very coarse or bimodal grain structure, like reaction-sintered SiC, the mirror and other fracture features may not be visible or distinct enough for measurement [26]. The fracture surface of the nodule itself was flat or smooth, which contrasted with the surrounding structure (Fig. 7b). This result corresponded well to that of the indentation microfracture shown in Fig. 6a. It is considered that the fracture strength of a reaction-sintered body can also be affected by a nodule. Unfortunately, we were unable to examine this because the control of the volume fraction of nodule was very difficult.

4. Conclusion

The fracture strength of the reaction-sintered SiC body decreased significantly with an increase in the volume fractions of the IFG β-SiC domain, and eventually fell to the strength of the β-SiC domain itself. The decrease in strength was most remarkable when the IFG β-SiC layer was situated at the tensile face. However, the fracture strength of the IFG β-SiC structure increased due to recrystallization by heat-treatment.

Crack deflections in the typical structure were generally more irregular than those in the IFG β-SiC structure, showing the decrease in fracture toughness due to the IFG β-SiC layer content.

The overall fractured face showed indistinct fracture features, even when the reaction-sintered SiC body contained the IFG β-SiC and nodules.

The decrease in both fracture strength and fracture toughness of the structure which contains the IFG β-SiC layer may be due to its small bonded area of grain boundary area and an imperfect bonding condition.

References

1. C. W. FORREST, P. KENNEDY and J. V. SHENNAN, "Special Ceramics 5" (British Ceramic Research Association, Stoke-on-Trent, 1972) p. 99.
2. H. SATO, S. SHINOZAKI, M. YESSIK and J. E. NOAKES, in Proceedings of Conference on silicon carbide, Miami Beach, 1973 (University of South Carolina Press, Columbia, South Carolina, 1974) p. 222.
3. S. SHINOZAKI, J. E. NOAKES and H. SATO, *J. Amer. Ceram. Soc.* **61** (1978) 237.
4. P. A. WILLERMENT, R. A. PETT and T. J. WHALEN, *Amer. Ceram. Soc. Bull.* **57** (1978) 744.
5. G. R. SAWYER and T. F. PAGE, *J. Mater. Sci.* **13** (1978) 885.
6. J. N. NESS and T. F. PAGE, *ibid.* **21** (1986) 1377.
7. R. PAMPUCH, E. WARASEK and J. BIALOSKORSKI, *Ceram Internat.* **12** (1986) 99.
8. C. B. LIM and T. ISEKI, *Adv. Ceram. Mater.* **3**(3) (1988) 291.
9. *Idem , ibid.*, to be published.
10. T. ISEKI, M. IMAI and H. SUZUKI, *Yogyo-Kyokai-shi* **91** (1983) 259.
11. P. POPPER, "Special Ceramics" (Heywood, London, 1960) p. 209.
12. T. ISEKI, T. YANO, M. IMAI and B. W. LIN, in "High Tech Ceramics", edited by P. Vincenzini (Amsterdam, 1987) p. 1003.
13. J. R. McLAREN, G. TAPPIN and R. W. DAVIDGE, *Proc. Br. Ceram. Soc.* **20** (1972) 259.
14. P. KENNEDY, J. V. SHENNAN, P. BRAIDEN, J. R. McLAREN and R. W. DAVIDGE, *ibid.* **22** (1973).
15. J. R. McLAREN, G. TAPPIN and R. W. DAVIDGE, *J. Mater. Sci.* **18** (1973) 1699.
16. D. R. CLARKE, *J. Amer. Ceram. Soc.* **62** (1979) 236.

17. K. T. FABER and A. G. EVANS, *ibid.* **66** (1983) 94.
18. R. W. DAVIDGE and T. J. GREEN, *J. Mater. Sci.* **3** (1968) 629.
19. R. M. FULRATH and J. A. PASK, "Ceramic Microstructures" (Wiley, New York, 1968) p. 343.
20. H. LIEBOWITZ, "Fracture", Vol. 5 (Academic, New York, 1972) p. 729.
21. R. W. DAVIDGE, "Mechanical Behaviour of Ceramics" (Cambridge University Press, London, 1979) p. 80.
22. M. GELL and E. SMITH, *Acta Metall.* **15** (1967) 253.
23. A. G. EVANS and E. A. CHARLES, *J. Amer. Ceram. Soc.* **59** (1976) 371.
24. K. NIIHARA, A. NAKAHIRA and T. HIRAI, *ibid.* **67** (1984) C1.
25. K. NIHARA, A. NAKAHIRA, T. UCHIYAMA and T. HIRAI, in "Fracture Mechanics of Ceramics", edited by R. G. Bradt (Plenum, New York, 1986) p. 103.
26. D. W. RICHERSON, "Modern Ceramic Engineering" (Dekker, New York, 1982) p. 329.

Received 7 September
and accepted 10 December 1987